JOURNAL OF MATERIALS SCIENCE 28 (1993) 6645–6649

Characteristics of thin nitrided oxides prepared by an *in-situ* process

SEOUNG HO LEE, MYOUNG GI SO
Department of Materials Engineering, Kang Won National University, 192-1 Hyojadong, Chuncheon, Kangwondo, 200-701, Republic of Korea

In this paper a new method of depositing silicon nitrided oxide by an *in-situ* process is introduced. Thin nitrided-oxide (NO) films were deposited on silicon by rapid thermal oxidation and rapid thermal chemical vapour deposition (RTCVD). Thin oxide films, 10.0 nm, were rapidly thermally grown in a dry oxygen ambient at 1000 °C and the silicon-nitride films were deposited on the oxide at 700–900 °C using an NH_3 and SiH_4 gaseous mixture. The effect of the NH_3/SiH_4 input ratio and the deposition temperature on the deposition rate and the electrical properties was studied. The experimental results show that the deposition rate increased with increasing deposition temperature and decreasing NH_3/SiH_4 input ratio. From the data for the Fourier-transform infrared spectroscopy (FTIR) and the *C–V* curves of the NO films, it was observed that the flat-band voltage is directly related to the N–H-bond peak intensity. The flat-band voltage shifts to the positive with increasing deposition temperature and to the negative with increasing NH_3/SiH_4 input ratio, and the breakdown field of NO films is higher than that of the RTP oxidation (RTO) films.

1. Introduction

Thin silicon-nitride films on thermally grown silicon oxide, which is a combination of stacked nitride/oxide (NO), can be formed by APCVD, LPCVD, PECVD, and thermal nitridation. Among these various techniques, chemical-vapour-deposition (CVD) methods are problematic in that they cannot successively form silicon nitride on thermally grown silicon oxide in a single chamber. On the other hand, NO films formed by thermal nitridation of thin SiO_2 have been investigated in the past few years and appear to be a promising dielectric for ULSI applications [1–2]. Thermal nitridation of thin oxides has been mostly achieved using conventional furnace techniques. But the nitridation of oxides has many problems when it is performed in furnaces, because the temperature required for the nitridation is so high that a considerable redistribution of impurity atoms occurs.

Recently, rapid thermal processing (RTP) has been proposed [3–4] as a solution to these problems and as an improvement in the quality of SiO_2 and of the thermal nitridation. In particular, it is well known that the NO films grown by RTP have several advantages [5–6] such as a reduction of the interface trap density and the blocking of impurity penetration into SiO_2 films. However, during the nitridation process, the inclusion of hydrogen-containing chemical species (such as $-NH_x$, $-H$, and $-OH$) into SiO_2, which contribute to the formation of electron traps [7] and a high fixed charge density [8], is unavoidable. Rapid thermal reoxidation of NH_3-nitrided SiO_2 has been proposed [9] to reduce the above species, but this process is rather complicated and is strongly dependent on the process conditions. To avoid these problems, this report focuses on the stacked growth of nitrided oxide films by RTP oxidation (RTO) and rapid-thermal-chemical-vapour-deposition (RTCVD) [10–11] technique. The RTCVD technique, also known as limited reaction processing [12], uses a continuous gas flow of appropriate precursors, in conjunction with the rapid heating and cooling capability of low-thermal-mass RTP equipment, to control the growth process. These advantages also allow formation of NO films by *in situ* multiple processing in a single chamber. Unfortunately, very little data has been reported on NO films formed by RTCVD.

The work reported here was undertaken to study the effects of the NH_3/SiH_4 input ratio and the deposition temperature on the deposition rate and on the electrical properties of NO films. Also, this study examines the correlation between the V_{FB} shift and, the N–H bond peak intensity, and, especially, the deposition temperature and input-gas-ratio dependences of both the V_{FB} shift (the flat-band voltage shift) and the N–H-bond peak intensity of the NO films formed by an *in-situ* process.

2. Experimental procedure

The RTCVD system used in this study consists of three main parts: the RTP reaction chamber, the exhaust system and the gas-distribution system, as shown in Fig. 1. The reaction chamber was fabricated from quartz. Ten tungsten halogen lamps were used to heat the wafer. The lamps were enclosed within a stainless-steel chamber which had a reflective coating

0022–2461 © *1993 Chapman & Hall*

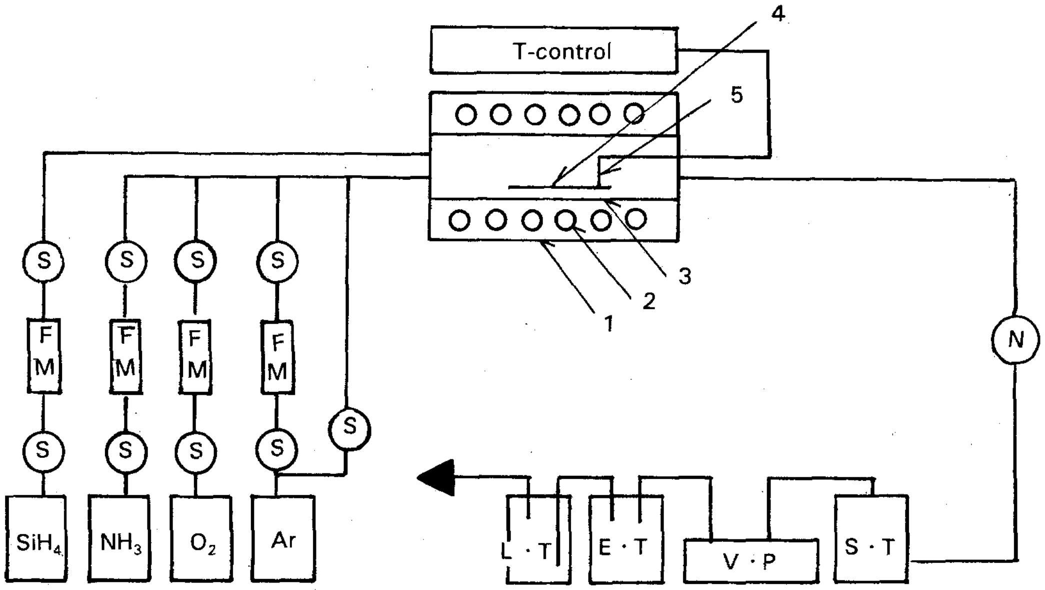

Figure 1 A schematic diagram of nitrided-oxide RTCVD apparatus. S, solenoid value; N, needle value; 1, reflector; 2, halogen lamp; 3, quartz tube; 4, silicon wafer; 5, thermocouple.

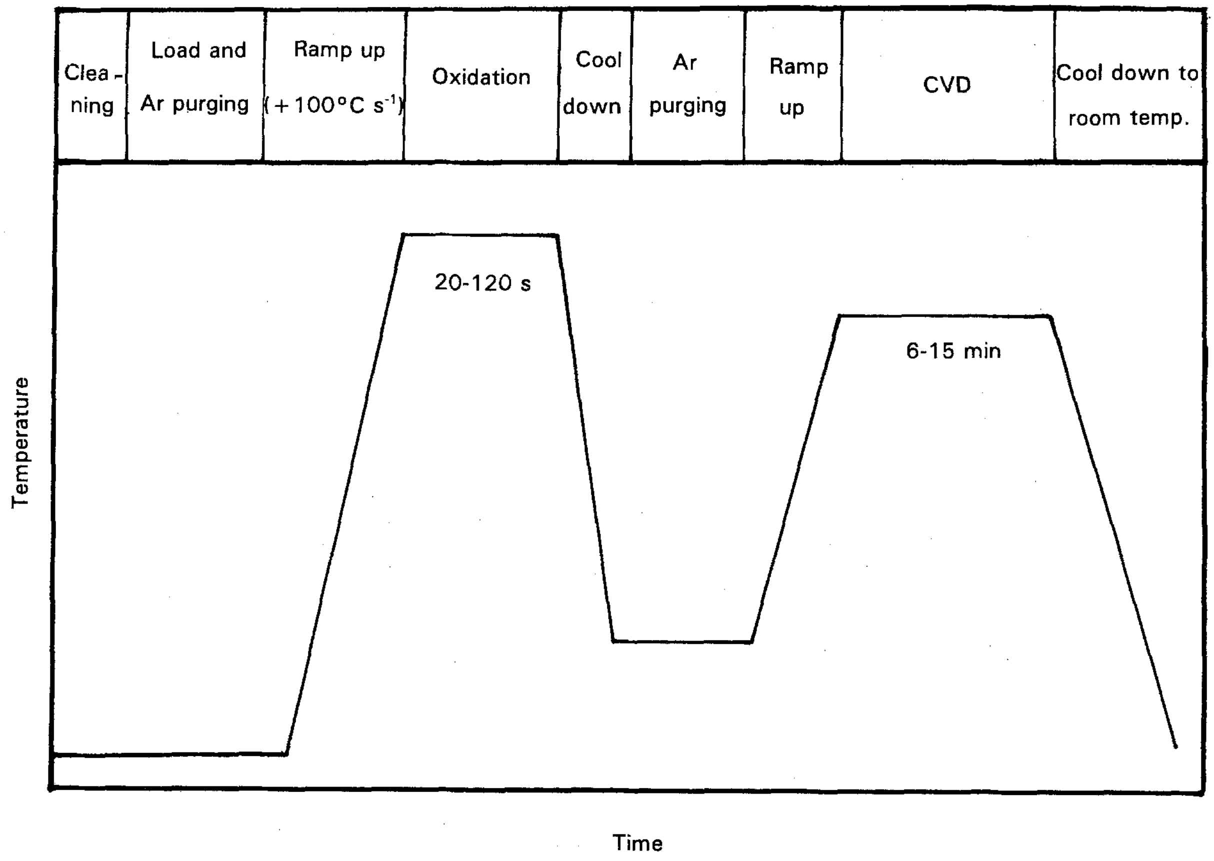

Figure 2 Experimental procedure of nitride-oxide film growth.

on the inner wall and was wafer cooled. The wafer temperature was measured by thermocouples. The operation of the RTP system was computer controlled. The desired temperature and time were obtained by a closed-loop system. An experimental procedure of NO film growth is shown schematically in Fig. 2. The substrate used in this experiment was a p-type (1 0 0) silicon wafer. All samples were HF dipped and rinsed in deionized water just prior to being loaded into the chamber. The chamber was purged with high-purity argon for about 3 min. After the Si wafers were purged, SiO$_2$ films 10 nm thick were rapid thermally grown in a dry O$_2$ ambient at 1000 °C. In sequence, RTCVD silicon nitride was deposited on the oxide by using a mixture of NH$_3$/SiH$_4$ gases at 700–900 °C in a range of the NH$_3$/SiH$_4$ input ratio change from 100 to 400. All experiments were performed at atmospheric pressure. The refractive indices and the thickness of the deposited films were measured by an ellipsometer. To characterize the chemical composition and the depth profile, the NO films were analysed by auger electron spectroscopy (AES). The functional groups, including hydrogen-containing bonds within the NO films, were measured by Fourier-transform infrared (FTIR) spectroscopy. The high-frequency (1 MHz) $C-V$ curves were also measured in order to determine the fixed charge densities from the flat-band voltage shift ΔV_{FB}. The reliability of the dielectric film was evaluated by the time-zero dielectric breakdown (TZDB).

3. Results and discussion

3.1. Effects of the deposition parameters

Fig. 3 shows the variation in the deposition rate and the refractive index of the NO films with the deposition temperature and the NH_3/SiH_4 input ratio.

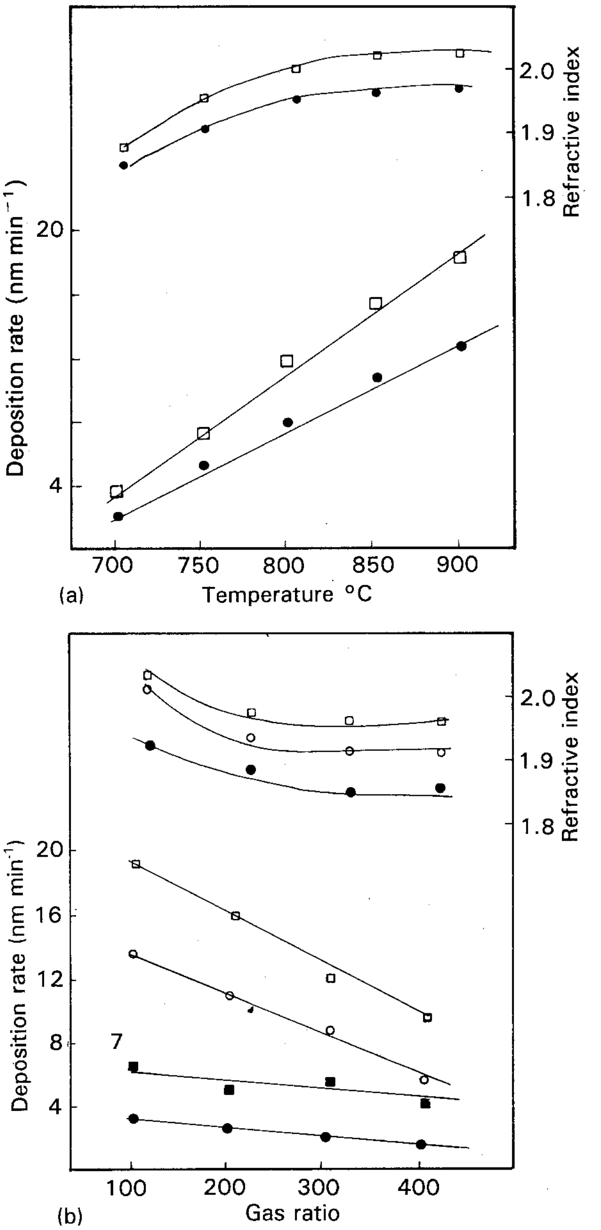

Figure 3 (a) Effects of the deposition temperature on the deposition rate and the refractive index (total pressure 1.01×10^5 Pa, SiH_4 = 4 s.c.c.m.), for the following NH_3/SiH_4 ratios: (●) 300, and (□) 100. (b) Effects of the NH_3/SiH_4 input gas ratio on the deposition rate and the refractive index, for the following temperatures: (●) 700 °C, SiH_4 = 4 s.c.c.m. (■) 700 °C, SiH_4 = 7 s.c.c.m. (○) 800 °C, and (□) 900 °C.

From Fig. 3a, it can be seen that the deposition rate increases with increasing temperature. The refractive index of the films increases with increasing temperature from 700 to 850 °C. However, the refractive index saturates at temperatures above 850 °C.

Fig. 3b shows that the deposition rate decreases with increasing NH_3/SiH_4 gas ratios at 700, 800 and 900 °C. The refractive index decreases with increasing gas ratios from 100 to 300; however, it saturates at ratios above 300.

It can be concluded from these results that the deposition rate increases with increasing deposition temperatures and decreasing NH_3/SiH_4 input ratios and the refractive index shows a constant value as the temperature and the NH_3/SiH_4 input ratio is increased. Also, it is likely that the total reaction rate is controlled by the silane ratio, because the deposition rate increases with increasing silane flow rate from 4 s.c.c.m. to 7 s.c.c.m. as shown in Fig. 3b.

3.2. Film composition

AES was used in conjunction with ion sputtering to determine the chemical composition and depth profile of the NO film deposited.

Fig. 4 shows the AES spectra for silicon nitride. It can be seen that for a silicon nitride layer deposited during the interaction of SiH_4 and NH_3 at 800 °C there are four groups of bands characterizing the following transitions: in silicon atoms, Si_{LVV} and Si_{KLL}; in nitrogen atoms, N_{KLL}; and in oxygen atoms, O_{KLL}. To obtain the depth profile, the amplitudes of the nitrogen, oxygen and silicon peaks were monitored continuously as a function of sputtering time.

Fig. 5 shows the AES depth profile for the NO film. The silicon and nitrogen concentrations increase in the surface region with increasing sputtering time, while the oxygen concentration decreases. In the interface region, the nitrogen and silicon concentrations decrease, while the oxygen concentration increases. The oxygen concentration in the silicon-nitride bulk region is due to contamination during the film deposition. It was also found that nitrogen is detected at the SiO_2/Si interface. As can be seen in Fig. 5 NO films form on the Si substrate.

Fig. 6 shows a typical FTIR absorption spectra of RTO and RTCVD silicon nitride. Fig. 6a shows that the FTIR absorption peak of oxide films grown for

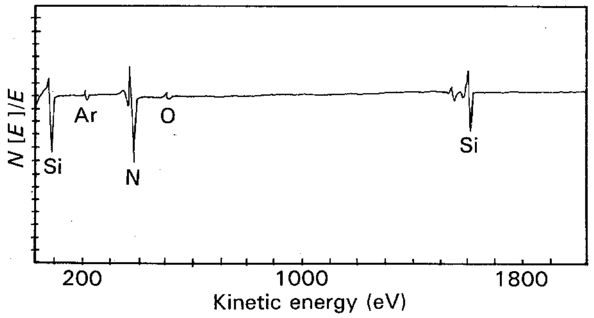

Figure 4 AES spectra of a nitride grown by RTCVD. (NH_3/SiH_4 input ratio = 300, temperature = 800 °C.)

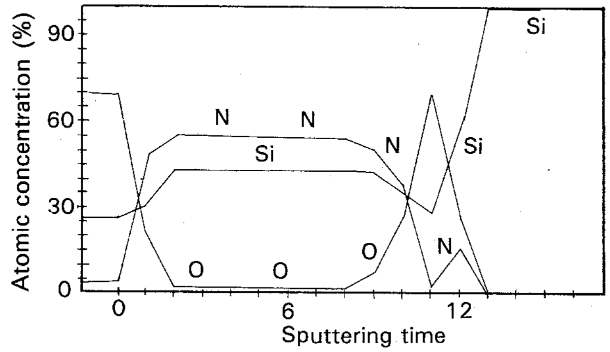

Figure 5 AES depth profile of a nitrided-oxide film.

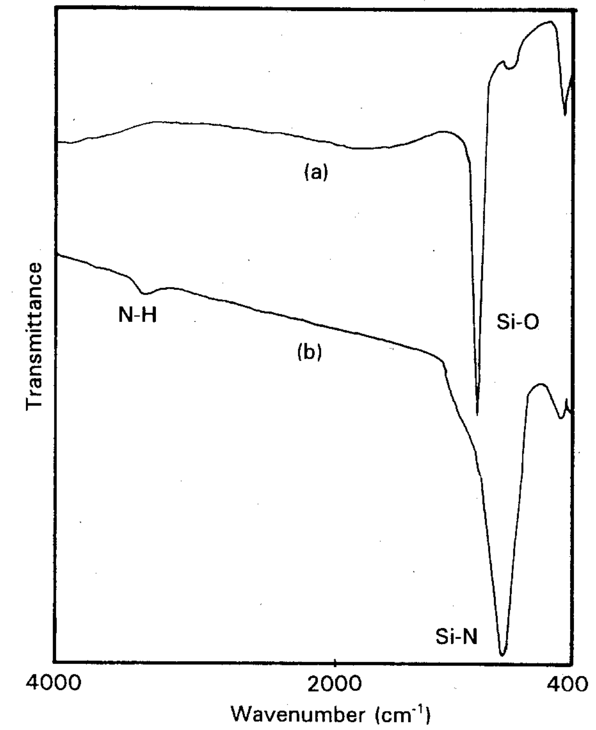

Figure 6 FTIR absorption spectra of (a) RTO, and (b) RTCVD nitride.

80 s at 1000 °C appears at 1072, 800 and 450 cm^{-1} [13]. The absorption peaks of Si_3N_4 films deposited for 480 s at 800 °C are shown in Fig. 6b. Notice that absorption peaks are observed for the Si–N bond at 868, 486 cm^{-1} and for the N–H bond at 3335 cm^{-1} [14], due to incomplete decomposition of NH_3 gas.

3.3. Electrical properties

The flat-band voltage, V_{FB}, was measured in order to understand the direct correlation between the fixed charge and the N–H-bond peak intensity. This was done by infrared (i.r.) measurement.

Fig. 7 shows the variation of the i.r. absorption and the high-frequency C–V curve shifts with the NH_3/SiH_4 input ratio at 900 °C. The V_{FB} shift towards the negative with increasing NH_3/SiH_4 input ratios can be seen in Fig. 7. This may be explained as follows: Pan [15] reported that nitridation introduces the N–H-bond, bringing about a negative flat-band shift. As shown in Fig. 7, the N–H-bond peak intensity increases with increasing input ratios. This result agrees well with those of Pan, although there is a difference in the nitride-growth method. Therefore, it can be concluded that, as the input ratio is increased, hydrogen bonding in the silicon nitride increases and the fixed charge becomes more and more positive, resulting in the negative shift of V_{FB}. Also, it was known that the amount of fixed charge was charged by the difference of hysteresis voltage. Although not quantitatively analysed, we found by measurement of the hysteresis voltage that the amount of the fixed charge increased as the input ratio was increased.

Fig. 8 shows the variation of the high-frequency C–V curve shift and the i.r. absorption with the deposition temperature at an NH_3/SiH_4 input ratio of 200. The V_{FB} shifted towards the positive when the deposition temperature increased from 700 to 900 °C. This may be explained as follows. As shown in Fig. 8, the N–H-bond peak intensity decreased when the deposition temperature increased from 700 to 900 °C.

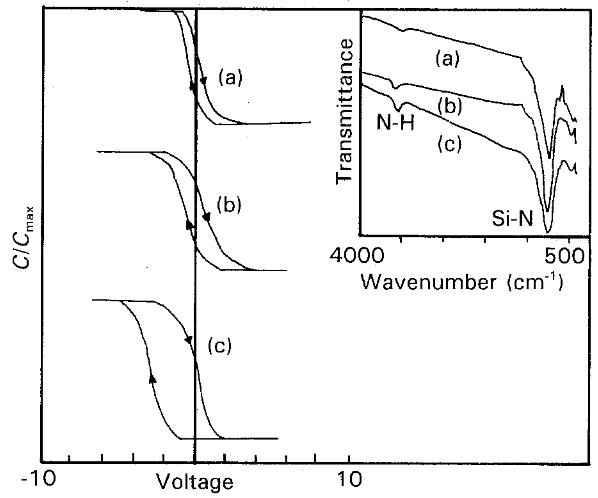

Figure 7 The variation of the i.r. absorption and the high-frequency C–V curve shifts with the NH_3/SiH_4 input ratio at 900 °C. (a) NH_3/SiH_4 input ratio = 100, (b) NH_3/SiH_4 input ratio = 200, (c) NH_3/SiH_4 input ratio = 300.

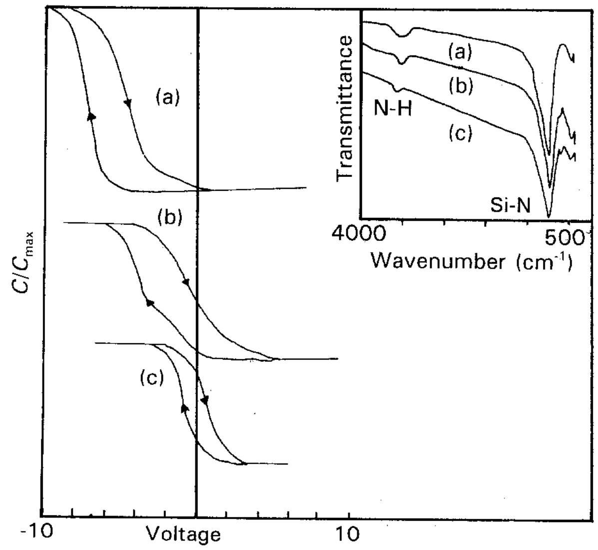

Figure 8 The variation of the i.r. absorption and the high-frequency C–V curve shifts with the deposition temperature at an NH_3/SiH_4 input ratio of 200. Deposition temperature = (a) 700 °C, (b) 800 °C, (c) 900 °C.

Chen *et al.* [16] and Ruggles and Monkowski [17] suggested that residual hydrogen plays an important role in generating a fixed-charge defect and that the observed decrease of the fixed charge density with increasing nitridation temperatures was due to a decrease in the hydrogen concentration at high temperatures. Therefore, from our result obtained by i.r., it is likely that the N–H-bond peak-intensity reduction with increasing temperature is due to the evolution of hydrogen from Si_3N_4 films deposited by RTCVD. As the deposition temperature is increased, the fixed charge is transformed from positive to negative. Consequently, we predict that the reduction of the N–H-bond peak intensity gives rise to the positive shift of V_{FB}.

Fig. 9 shows the variation of the fixed charge of the deposited film after annealing at 1000 °C in an Ar ambient for 20 min. It can be seen from Fig. 9 that the fixed charge is remarkably reduced after annealing. This can also be explained by the variation of the N–H-bond peak intensity. After annealing, the N–H-bond peak intensity decreased. This, therefore, implies that the reduction of the fixed charge corresponds to the reduction of the N–H-bond peak intensity.

The reliability of an RTO and NO film breakdown field was measured by TZDB. Fig. 10 shows breakdown histograms for both RTO (1000 °C) and RTCVD grown (800 °C) NO films. It can be seen from Fig. 10 that the breakdown field of NO films is higher than that of the RTO films.

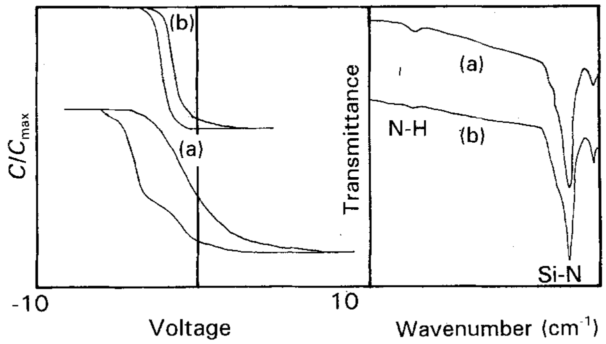

Figure 9 The variation of the fixed charge of the deposited film after annealing at 1000 °C. (a) Deposition temperature = 800 °C, NH_4/SiH_4 input ratio = 200, (b) at 1000 °C, 20 min annealing.

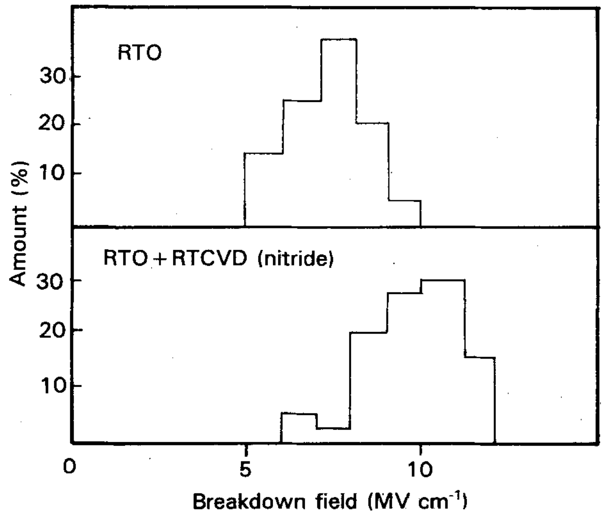

Figure 10 Breakdown histograms for both RTO and nitrided-oxide films.

4. Conclusions

1. The deposition rate increase with increasing deposition temperatures and decreasing NH_3/SiH_4 input ratios. The refractive index saturated the constant value with increases in both the temperature and the NH_3/SiH_4 input ratio.

2. The V_{FB} shifted to the positive with the increasing deposition temperatures and to the negative with increasing NH_3/SiH_4 input ratios; this is related to the variation of the N–H-bond peak intensity.

3. After annealing, a reduction of the fixed charge, which is due to the reduction of the N–H-bond peak intensity, was observed.

4. The value of the electrical breakdown field of the NO films was higher than that of the RTO films.

Acknowledgements

The authors acknowledge the support of the Korean Research Foundation which made this work possible.

References

1. T. ITO, T. NAKAMURA and H. ISHIKAWA, *J. Electrochem. Soc.* **129** (1982) 184.
2. C. T. CHEN, F. Y. CHANG and M. K. LEE, *ibid.* **131** (1984) 875.
3. H. FUKUDA, T. IWABUCHI and S. OHNO, *Jpn. J. Appl. Phys.* **27** (1988) L2164.
4. W. T. CHANG, D. K. SHIH and D. L. KWONG, *Appl. Phys. Lett.* **54** (1989) 430.
5. M. M. MOSLEHI and K. C. SARASWAT, *IEEE Trans. Electron Devices* **32** (1985) 106.
6. T. HORI and H. IWASAKI, *IEEE Electron Devices Lett.* **10** (1989) 64.
7. T. HORI, H. IWASAKI and K. TSUJI, *IEEE Trans. Electron Devices* **35** (1988) 904.
8. Y. NAITO, T. HORI, H. IWASAKI and H. ESAKI, *J. Vac. Sci. Technol. B* **5** (1987) 633.
9. H. FUKUDA, T. ARAKAWA and S. OHNO, *IEEE Trans. Electron Devices* **39** (1992) 127.
10. M. L. GREEN, D. BRASEN, and H. LUFTMAN, *J. Appl. Phys.* **65** (1989) 2558.
11. A. J. STECKL and J. P. LI, *IEEE Trans. Electron Devices* **39** (1992) 64.
12. J. C. STURM, C. M. GRONET and J. F. GIBBONS, *J. Appl. Phys.* **59** (1986) 4180.
13. G. LUCOVSKY, P. D. RICHARD and D. V. TSU, *J. Vac. Sci. Technol. A* **4** (1986) 681.
14. R. C. BUDHANI, S. PRAKASH and H. J. DOERR, *ibid. A* **5** (1987) 1644.
15. P. PAN, *J. Appl. Phys.* **61** (1987) 284.
16. C. T. CHEN, F. C. TSENG and C. Y. CHANG, *J. Electrochem. Soc.* **131** (1984) 875.
17. G. A. RUGGLES and J. R. MONKOWSKI, *ibid.* **133** (1986) 787.

Received 30 July 1992
and accepted 3 June 1993